Applied Catalysis B: Environmental 89 (2009) 295–302

Contents lists available at ScienceDirect

Applied Catalysis B: Environmental

journal homepage: www.elsevier.com/locate/apcatb

VOC oxidation over $CuO–CeO_2$ catalysts prepared by a combustion method

Dimitrios Delimaris [a,b], Theophilos Ioannides [a,*]

[a] Foundation for Research and Technology-Hellas, Institute of Chemical Engineering and High Temperature Chemical Processes (FORTH/ICE-HT), P.O. Box 1414, GR-26504 Patras, Greece
[b] Department of Chemistry, University of Patras, GR-26504 Patras, Greece

ARTICLE INFO

Article history:
Received 7 November 2008
Received in revised form 30 January 2009
Accepted 9 February 2009
Available online 20 February 2009

Keywords:
VOC
Oxidation
Ethanol
Ethyl acetate
Toluene
Ceria
Copper oxide

ABSTRACT

$CuO–CeO_2$ catalysts were prepared via a urea combustion method and their performance in the oxidation of ethanol, ethyl acetate and toluene was evaluated. XRD, H_2-TPR and N_2 physisorption were employed in catalyst characterization. The specific surface area of mixed materials was higher than the one of single oxides. In ceria-rich materials, crystalline copper oxide phases are absent and segregation of a CuO phase takes place at atomic Cu/(Cu + Ce) ratios higher than 0.25. The mixed oxides get reduced by H_2 at lower temperatures than the corresponding single oxides and copper ions promote reduction of ceria. Ethanol gets more easily oxidized than ethyl acetate, which in turn gets more easily oxidized than toluene. $CuO–CeO_2$ catalysts of low copper content produce very low amounts of acetaldehyde during ethanol and ethyl acetate oxidation at all conversion levels. This is augmented by the presence of water in the feed. The specific activity of Cu_xCe_{1-x} catalysts in the oxidation of ethanol, ethylacetate and toluene (specific rate of volatile organic compound (VOC) consumption) is lower than the one of pure CuO and CeO_2, i.e. combination of the two phases leads to suppression of intrinsic activity. On the other hand, the specific rate of CO_2 production during ethanol and ethyl acetate oxidation is also lower over $CuO–CeO_2$ than over CeO_2, but higher than over CuO. The larger surface area of $CuO–CeO_2$ catalysts counterbalances their smaller specific activity allowing complete VOC conversion at lower temperatures compared to the single oxides.

1. Introduction

Volatile organic compounds (VOCs), emitted from a variety of industrial processes and transportation activities, are considered as an important class of air pollutants. Catalytic oxidation is one of the most developed techniques used for the elimination of VOCs, as it requires lower temperatures than thermal oxidation [1,2]. Typical catalysts for VOC oxidation are mainly noble metals, which show high activity at low temperatures [2–6], but they are costly and have low stability in the presence of chloride compounds [7]. Metal oxides (Fe, Cr, Cu, Mn and Co) are a cheaper alternative to noble metals as catalysts for VOC oxidation [8–11]. They present sufficient activity, although they are less active than noble metals at low temperatures. $CuO–CeO_2$ mixed metal oxides comprise a promising family of catalysts and have been studied by many investigators in reactions, such as, the combustion of CO and CH_4 [12–14], the water–gas shift reaction [15], the reduction of NO [16], decomposition of H_2O_2 [17] and the wet oxidation of phenol [18]. The high activity of $CuO–CeO_2$ is attributed to the promoting effect of ceria due to its high oxygen storage capacity and facile Ce^{4+}/Ce^{3+} redox cycle. Several methods for the preparation of $CuO–CeO_2$ catalysts have been reported, such as combustion [17], thermal decomposition [19], sol–gel [20], co-precipitation [21] and impregnation [22].

Although $CuO–CeO_2$ materials are effective oxidation catalysts, their performance in VOC oxidation has been scarcely examined. Larsson and Andersson [1] have studied the oxidation of ethanol and ethyl acetate over CuO/TiO_2 and $CuO–CeO_2/TiO_2$ catalysts. Hu et al. [23] have reported on the high activity of a $CuO–CeO_2$ (10 at.% Cu) catalyst in benzene oxidation. In the present work several $CuO–CeO_2$ catalysts have been prepared via the combustion method and their catalytic performance was examined in the oxidation of ethanol, ethyl acetate and toluene. Catalysts were characterized by XRD, H_2-TPR and N_2 physisorption.

2. Experimental

2.1. Catalyst preparation

$CuO–CeO_2$ catalysts with varying copper content were synthesized via the urea–nitrate combustion method, using urea and nitrate salts as starting compounds. The reactions describing the

* Corresponding author.
E-mail address: theo@iceht.forth.gr (T. Ioannides).

0926-3373/$ – see front matter © 2009 Elsevier B.V. All rights reserved.
doi:10.1016/j.apcatb.2009.02.003

combustion of urea with copper and cerium nitrate salts can be written as follows:

$$Ce(NO_3)_3 + (7/3)CO(NH_2)_2 \rightarrow CeO_2 + (23/6)N_2 + (7/3)CO_2 + (14/3)H_2O \quad (1)$$

$$Cu(NO_3)_2 + (5/3)CO(NH_2)_2 \rightarrow CuO + (8/3)N_2 + (5/3)CO_2 + (10/3)H_2O \quad (2)$$

The stoichiometric ratio of urea to the metal salt is 2.33 for cerium and 1.67 for copper, while it takes values in the range of 1.67–2.33 for a mixed Cu–Ce oxide. In the present work, the amount of urea was higher than stoichiometry with equivalence ratio Φ (Φ = actual urea/stoichiometric urea) in the range 3.0–7.3. A mixed solution of urea and nitrate salts of copper and cerium, in the appropriate molar ratios was autoignited in an open muffle furnace (pre-heated at 500 °C). The powders were further calcined at 550 °C for 2 h in order to remove any remaining carbon residues. Details of the synthesis procedure have been reported elsewhere [11,12]. Catalysts are denoted as Cu_xCe_{1-x}, where x is the Cu/(Cu + Ce) atomic ratio.

2.2. Catalyst characterization

The specific surface area and pore size distribution of the samples were determined by N_2 adsorption at −196 °C in an automated apparatus (Autosorb-1, Quantachrome Corporation). Prior to measurement, the samples were outgassed at 150 °C for 2 h. The surface area was calculated via the BET equation, while the BJH method was employed for calculating the pore size distribution from the desorption branch of the isotherms. The crystalline structure of the catalysts was analyzed by means of an X-ray powder diffractometer (D8 Advance Bruker AXS) employing Cu Kα radiation (λ = 0.15418 nm) and a Lynx Eye Position Sensitive Detector. The scan speed during analysis was 2 s/step. The mean crystallite diameter was determined by means of the Scherrer's equation [24]. Temperature-programmed reduction (TPR) experiments were performed under a flow of a 3% H_2/He mixture (50 cm^3 min^{-1}) with a heating rate of 10 °C min^{-1}. Prior to TPR, the catalysts were treated under a 20% O_2/He mixture at 400 °C for 15 min. A mass spectrometer (Omnistar/Pfeiffer Vacuum) was used for on-line monitoring of TPR effluent gas. The sample weight was in the range of 16–254 mg depending on the copper content of the catalysts. The above weight range was chosen based on the methodology for optimal selection of experimental parameters in a TPR run [25,26].

2.3. Catalytic activity tests

Catalytic activity tests were carried out in a conventional flow reactor at atmospheric pressure using 60 mg of catalyst with particle size in the range 90–180 μm. Prior to all catalytic tests, the samples were heated in a flowing 20 vol.% O_2/He mixture at 300 °C for 15 min as a standard pretreatment, followed by cooling down to the reaction temperature in pure He. The total flow rate of the reaction mixture was 50 cm^3 min^{-1} corresponding to a W/F ratio of 0.072 g s cm^{-3} or a space velocity of 50,000 h^{-1}. Ethanol, ethyl acetate and toluene were chosen as representative VOCs and were introduced in the reactor feed with the aid of a small, controlled helium flow passing through saturators kept at room temperature. The VOC-loaded helium flow was subsequently mixed with the main air feed to the reactor. The VOC concentration in the air feed was: 1600 ppm (ethanol), 1800 ppm (ethyl acetate), 600 ppm (toluene). The effluent gases were analyzed by a gas chromatograph (Shimadzu GC-14B) equipped with TCD and FID and two gas sampling valves. The employed chromatographic columns were: Porapak QS (analysis of organics) and Carboxen (analysis of CO_2) with dimensions 1/8 in. OD × 1.5 m length. The conversion (X) of VOCs was calculated using the following equation:

$$X = \frac{C_{in} - C_{out}}{C_{in}} \quad (3)$$

where C_{in} and C_{out} are the feed and outlet concentration of the specific VOC, respectively. The conversion (yield) to CO_2 was calculated as given below:

$$X_{CO_2} = \frac{C_{CO_2\,out}/n}{C_{VOC\,in}}, \quad (4)$$

where n is the carbon number of VOC molecule

The conversion to acetaldehyde and ethylacetate in the case of ethanol oxidation was calculated from Eqs. (5) and (6), respectively:

$$X_{acetaldehyde} = \frac{C_{acetaldehyde\,out}}{C_{EtOH\,in}} \quad (5)$$

$$X_{ethylacetate} = \frac{2C_{ethylacetate\,out}}{C_{EtOH\,in}} \quad (6)$$

In the case of ethyl acetate oxidation, conversion to ethanol, acetaldehyde or acetic acid was calculated from Eq. (7):

$$X_i = \frac{C_{i\,out}}{2C_{EAc\,in}}, \quad (7)$$

where i is the ethanol, acetaldehyde or acetic acid.

The reproducibility of catalytic experiments was verified by testing different batches of the $Cu_{0.15}Ce_{0.85}$ catalyst.

3. Results and discussion

3.1. Effect of urea equivalence ratio Φ

The amount of urea employed during synthesis affects the catalyst structure, as it helps to control the temperature increase during autoignition [11,12]. In order to identify the catalyst with optimal catalytic properties, several $Cu_{0.15}Ce_{0.85}$ catalysts were synthesized by varying the urea equivalence ratio, Φ. Table 1 presents the BET specific surface areas, S_{BET}, and pore volume, V_p, of $Cu_{0.15}Ce_{0.85}$ catalysts prepared with different Φ ratios. The specific surface area and pore volume is maximized at Φ = 5.19 and 6.10. The catalytic activity of $Cu_{0.15}Ce_{0.85}$ catalysts was examined in ethanol oxidation (Fig. 1) and it was found that the highest catalytic activity is also obtained for catalysts prepared with Φ ratios of 5.19 and 6.10. The observed catalytic behavior is in agreement with surface area measurements. All results presented thereafter refer to catalysts prepared using Φ = 5.19.

3.2. Catalyst characterization

The isotherms of nitrogen adsorption/desorption were of type II and had type B hysteresis loops closing at P/P_0 = 0.4 for all catalysts. The pore size distribution, as estimated using the BJH method, was very broad indicating that the catalysts have pores of various sizes

Table 1
Specific surface area, S_{BET}, and pore volume, V_p, of $Cu_{0.15}Ce_{0.85}$ catalysts prepared with varying urea equivalence ratios, Φ.

Φ	S_{BET} (m^2 g^{-1})	Pore volume (cm^3 g^{-1})
3.05	10.3	0.08
4.12	19.7	0.16
5.19	52.9	0.22
6.10	51.2	0.18
7.32	27	0.13

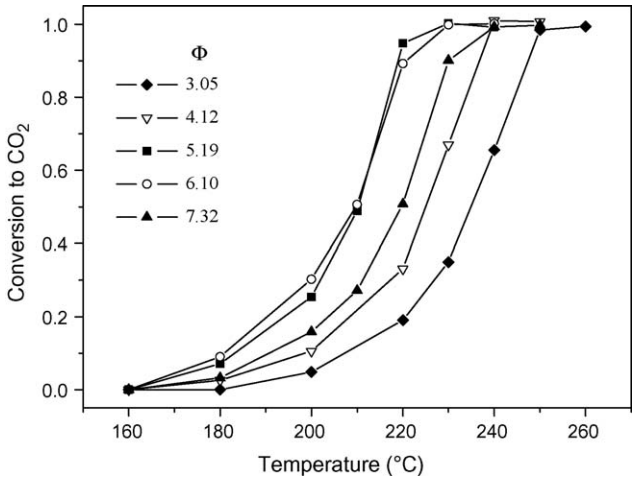

Fig. 1. Effect of urea equivalence ratio, Φ, employed in synthesis of $Cu_{0.15}Ce_{0.85}$ catalyst on its activity in ethanol oxidation.

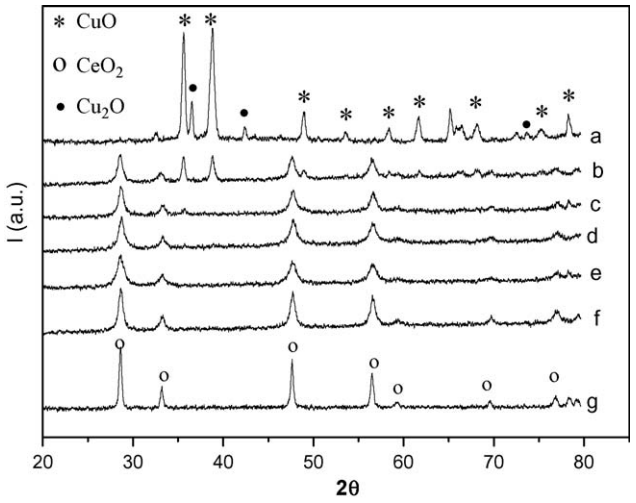

Fig. 2. XRD patterns of catalysts: (a) CuO; (b) $Cu_{0.75}Ce_{0.25}$; (c) $Cu_{0.5}Ce_{0.5}$; (d) $Cu_{0.25}Ce_{0.75}$; (e) $Cu_{0.15}Ce_{0.85}$; (f) $Cu_{0.05}Ce_{0.95}$; (g) CeO_2.

starting from ~2 to 3 nm and extending well into the macropore region. The specific surface area (S_{BET}) and the total pore volume (V_p) of the samples are presented in Table 2. As it is shown, all Cu_xCe_{1-x} catalysts have a specific surface area in the range of 11–53 $m^2\,g^{-1}$, which is higher than the one of pure CeO_2 and CuO (~5 and ~2.5 $m^2\,g^{-1}$, respectively), implying that the interaction of the two oxides enhances the surface area of the final material. The largest surface area and pore volume are observed for the $Cu_{0.15}Ce_{0.85}$ catalyst. Further increase of copper loading leads to smaller values of surface area and pore volume in accordance to what has been found previously [19,27,28]. Generally, we have found that use of the combustion method leads to CuO–CeO_2 materials with surface areas up to ~50 $m^2\,g^{-1}$. Higher surface areas may be obtained by co-precipitation, although the actual surface area values, in this case, are strongly dependent on catalyst calcination temperature and on parameters of co-precipitation. Hu et al. [23], for example, reported a surface area of 164.6 $m^2\,g^{-1}$ for a CuO–CeO_2 catalyst prepared by co-precipitation in the presence of NH_4NO_3 and surfactants. In the case of CuO–CeO_2 catalysts prepared by impregnation, the surface area of the final catalyst is comparable to the surface area of the parent ceria support. Surface area comparisons of CuO–CeO_2 catalysts prepared by various methods can be found in Refs. [29,42].

Fig. 2 presents the XRD patterns of Cu_xCe_{1-x} catalysts. A fluorite-type oxide structure of CeO_2 is present in all samples, but no reflections of a copper oxide phase are found in catalysts with atomic ratio Cu/(Cu + Ce) < 0.5, which is in agreement with previous studies [17,27,29]. The missing CuO phase in XRD patterns may be attributed to fine dispersion of CuO particles on the surface of ceria [16,28,30,31] or the formation of an interfacial solid solution [19,21]. In the case of $Cu_{0.50}Ce_{0.50}$ and $Cu_{0.75}Ce_{0.25}$ samples, reflections of the CuO phase are present in addition to those of ceria, as the increase in copper content leads to the formation of bulk CuO particles which are detected by XRD. It has to be mentioned that no observable shift in the diffraction lines of CeO_2 could be found in any of the catalysts. In the case of pure copper oxide the main phase is CuO, while the reflections at $2\theta = 36.7^\circ$, 42.5° and 73.9° can be attributed to a Cu_2O phase. The presence of a Cu_2O phase on a copper oxide catalyst prepared via the combustion method has been reported previously by Rao et al. [17], who have found that it is possible to vary the relative amounts of CuO and Cu_2O phases by changing the fuel content. The crystallite size of CeO_2 was calculated from XRD data by the Scherrer equation and the results are presented in Table 2. Pure CeO_2 has a crystallite size of 82 nm, but it decreases considerably to 8–15 nm in the case of Cu_xCe_{1-x} catalysts. This is in qualitative agreement with BET measurements.

TPR profiles of pure copper oxide and Cu_xCe_{1-x} catalysts are presented in Fig. 3, which depicts the water concentration in the reactor effluent as a function of temperature (the profile of water was identical to that of consumed hydrogen). The TPR profile of pure CeO_2 is not included, as it showed negligible hydrogen consumption below 600 °C. Reduction of pure copper oxide commences at ~200 °C and is characterized by two overlapping peaks at 268 and 323 °C. The first peak (at 268 °C) can be attributed to the reduction of Cu_2O species and the second one to the reduction of CuO particles. This is in agreement with Wang et al. [32] who found that Cu_2O is more easily reduced than CuO. Moreover many studies until now have reported that a single reduction peak is observed during reduction of pure CuO

Table 2
Physicochemical characteristics of Cu_xCe_{1-x} catalysts.

Sample	S_{BET} ($m^2\,g^{-1}$)	$d_{(1\,1\,1)}$[a] (nm)	V_p ($cm^3\,g^{-1}$)	Amounts of produced water during H_2-TPR		% reduction $Ce^{4+} \rightarrow Ce^{3+}$
				mmol H_2O/g_{cat}	mmol H_2/g_{cat} (theoretical values)	
CeO_2	4.8	82.1	0.06	~0	nd	–
$Cu_{0.05}Ce_{0.95}$	37.4	14.8	0.13	0.77	0.30	17
$Cu_{0.15}Ce_{0.85}$	52.9	8.4	0.23	1.40	0.95	17
$Cu_{0.25}Ce_{0.75}$	47.1	11.7	0.18	2.46	1.68	31
$Cu_{0.5}Ce_{0.5}$	21.8	12.6	0.09	4.26	3.98	15
$Cu_{0.75}Ce_{0.25}$	10.9	13.7	0.05	7.75	7.31	36
CuO	2.5	22.0	0.06	11	12.5	–

[a] All column data correspond to ceria crystallite size, with the exception of the last value, which corresponds to crystallite size of CuO.

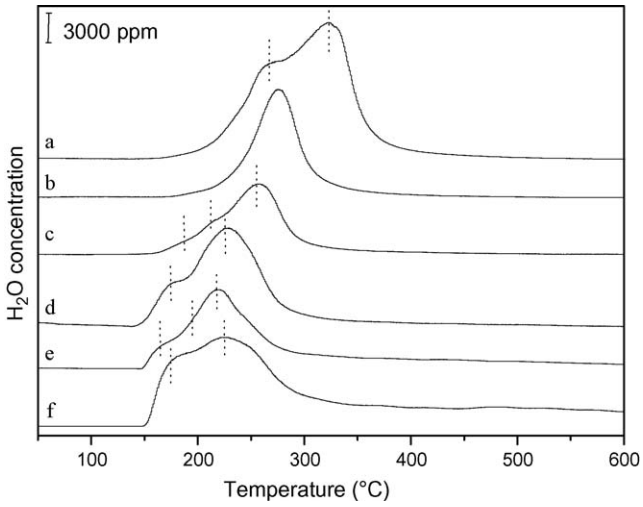

Fig. 3. TPR profiles of catalysts: (a) CuO; (b) $Cu_{0.75}Ce_{0.25}$; (c) $Cu_{0.5}Ce_{0.5}$; (d) $Cu_{0.25}Ce_{0.75}$; (e) $Cu_{0.15}Ce_{0.85}$; (f) $Cu_{0.05}Ce_{0.95}$.

[19,29,33], which shows that the presence of two reduction peaks is an evidence of the existence of Cu^+ species. Quantitative analysis of TPR runs (Table 2) revealed that the total water production was lower than the value expected if all copper in the sample was present as CuO.

The reduction of Cu_xCe_{1-x} catalysts takes place at lower temperatures than pure CuO and presents the following characteristics: (i) there are at least two overlapping peaks in catalysts with low copper content up to 0.25, in accordance to what has been found by others [20,34–38] and (ii) further increase of copper content leads to gradual disappearance of the low-temperature peak and shift of the main peak to higher temperatures. Quantitative analysis of TPR runs, the results of which are given in Table 2, shows that the amount of water produced during TPR is larger than the theoretical values corresponding to reduction of CuO to Cu^0, i.e. reduction of ceria takes place concurrently with CuO reduction. The extent of ceria reduction varies in the range of 15–36%. Caputo et al. [39] have measured the excess hydrogen uptake due to ceria reduction during TPR of CuO/CeO_2 to range from 200 to 250 $\mu mol\ g^{-1}$ corresponding to a reduction extent of 7–9%. The observed difference in the reduction extent may be attributed to the different catalyst preparation method employed in Ref. [39]. The reduction of ceria alongside CuO reduction certainly complicates allocation of TPR peaks to reduction of specific CuO moieties. The low-temperature reduction peak is generally attributed to highly dispersed, amorphous CuO clusters strongly interacting with the CeO_2 support, while the higher temperature peaks are due to reduction of larger CuO particles and concurrent reduction of ceria. The change in shape and position of TPR profiles for catalysts with high copper content correlates to the appearance of bulk-like crystalline CuO, as found by XRD.

3.3. Catalytic performance in VOC oxidation

The catalytic performance of CuO, CeO_2 and Cu_xCe_{1-x} catalysts was evaluated in the oxidation of ethanol, ethyl acetate and toluene. The conversion of ethanol to CO_2 as a function of temperature is presented in Fig. 4. The least active catalyst is CuO followed by CeO_2. All Cu_xCe_{1-x} catalysts achieve complete conversion of ethanol at lower temperatures than the pure oxides. Addition of copper oxide to ceria leads to more active catalysts up to a Cu content of 25 at.%. Further increase of copper content diminishes catalytic activity. The most active catalysts are $Cu_{0.15}Ce_{0.85}$ and $Cu_{0.25}Ce_{0.75}$, which show similar behavior,

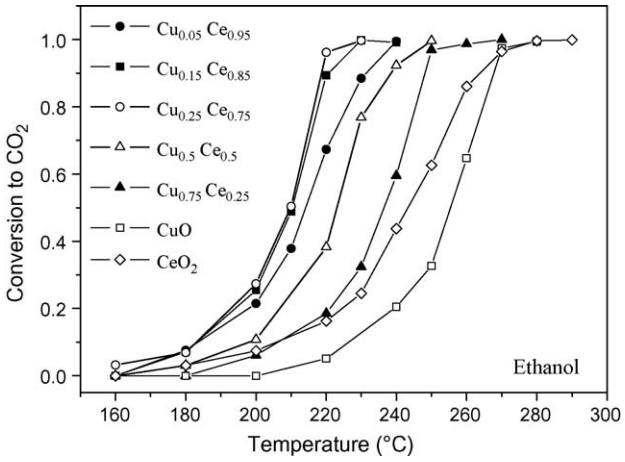

Fig. 4. Conversion of ethanol to CO_2 as a function of reaction temperature.

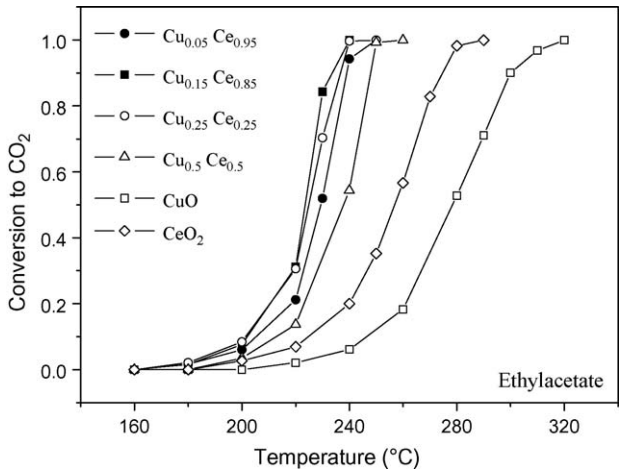

Fig. 5. Conversion of ethyl acetate to CO_2 as a function of reaction temperature.

achieving complete ethanol conversion to CO_2 at 220 °C, while pure CuO and CeO_2 require temperatures above 280 °C.

The conversion of ethyl acetate and toluene to CO_2 as a function of temperature is presented in Figs. 5 and 6, respectively. The observed trend is similar to the one found in the case of ethanol oxidation with $Cu_{0.15}Ce_{0.85}$ and $Cu_{0.25}Ce_{0.75}$ being again the most

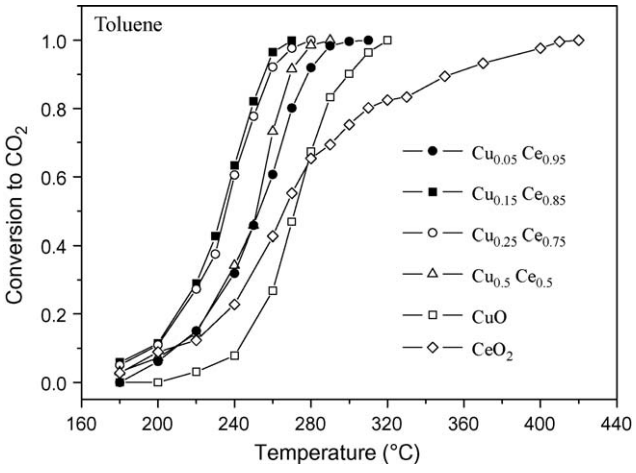

Fig. 6. Conversion of toluene to CO_2 as a function of reaction temperature.

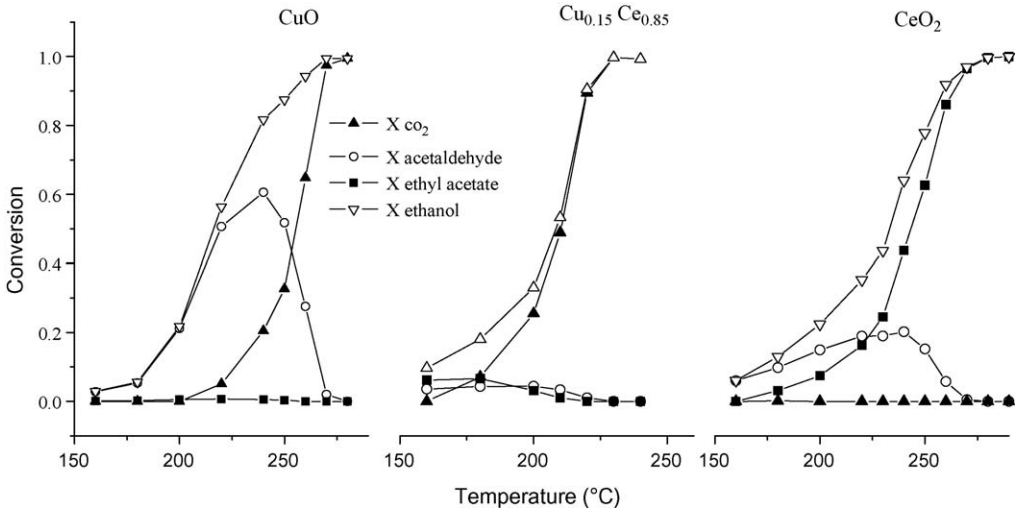

Fig. 7. Intermediate products of ethanol oxidation over CeO_2, $Cu_{0.15}Ce_{0.85}$ and CuO catalysts.

active catalysts. Ethyl acetate and toluene get less easily oxidized than ethanol: complete conversion of ethyl acetate and toluene to CO_2 over the $Cu_{0.15}Ce_{0.85}$ catalyst takes place at 240 and 260 °C, respectively. CeO_2 has comparable activity to the other catalysts in toluene oxidation at low temperatures, but complete conversion of toluene requires temperatures higher than 400 °C. At this stage, we do not have any plausible explanation for the "peculiar" behavior of CeO_2 in toluene oxidation.

The intermediate products of ethanol oxidation over Cu_xCe_{1-x} catalysts were found to be acetaldehyde and ethyl acetate. Fig. 7 presents the conversion of ethanol to acetaldehyde, ethyl acetate and CO_2 over CeO_2, $Cu_{0.15}Ce_{0.85}$ and CuO catalysts. In the case of pure CuO, acetaldehyde is the single product of the reaction at low temperatures. CeO_2 produces also acetaldehyde at low temperatures, but the maximum conversion to acetaldehyde is lower than the one over CuO. Cu_xCe_{1-x} catalysts produce lower amounts of acetaldehyde than the pure oxides. A minimum in acetaldehyde selectivity is observed over the $Cu_{0.15}Ce_{0.85}$ catalyst, while further increase of catalyst copper content leads to progressive increase of the amount of produced acetaldehyde. Ethyl acetate, on the other hand, is produced in trace amounts over the pure oxides but its production is higher over Cu_xCe_{1-x} catalysts. The presence of ethyl acetate in the reaction products indicates that acetate species are formed on the catalysts surface and they subsequently combine with adsorbed ethanol in an esterification reaction. Larsson and Andersson [1] have observed acetaldehyde as a major and ethyl acetate as a minor intermediate product during ethanol oxidation over CuO/TiO_2 and $CuO–CeO_2/TiO_2$ catalysts. Addition of CeO_2 to CuO/TiO_2 leads to a small decrease in the yield of acetaldehyde from ~31% to 27%. Our results suggest a more drastic effect of ceria addition to CuO on acetaldehyde selectivity.

The intermediate products during ethyl acetate oxidation were ethanol, acetaldehyde and acetic acid. Fig. 8 depicts the conversion of ethyl acetate to these products over CeO_2, $Cu_{0.15}Ce_{0.85}$ and CuO catalysts. The observed product distribution indicates that ethyl acetate is initially decomposed to ethanol and acetic acid. Acetic acid appears only in trace amounts in the reaction products and is preferentially oxidized with respect to ethanol due to its stronger adsorption on the surface [11]. Acetaldehyde is formed by partial oxidation of ethanol. The relative amounts of acetaldehyde and ethanol are determined by the selectivity of the specific catalyst towards acetaldehyde production from ethanol (see Fig. 4). Thus, in the case of CuO, the main intermediate product is acetaldehyde, while the main intermediate is ethanol over CeO_2 and ethanol is almost exclusively produced over $Cu_{0.15}Ce_{0.85}$. The results of the present work are qualitatively similar to what has been found in Ref. [1] concerning ethyl acetate oxidation over CuO/TiO_2 and $CuO–CeO_2/TiO_2$, although, in our case, there are pronounced differences in the relative amounts of ethanol and acetaldehyde produced over CuO and $Cu_{0.15}Ce_{0.85}$ catalysts.

The influence of the presence of H_2O or CO_2 in the VOC/air feed was evaluated with catalytic tests performed with the most active

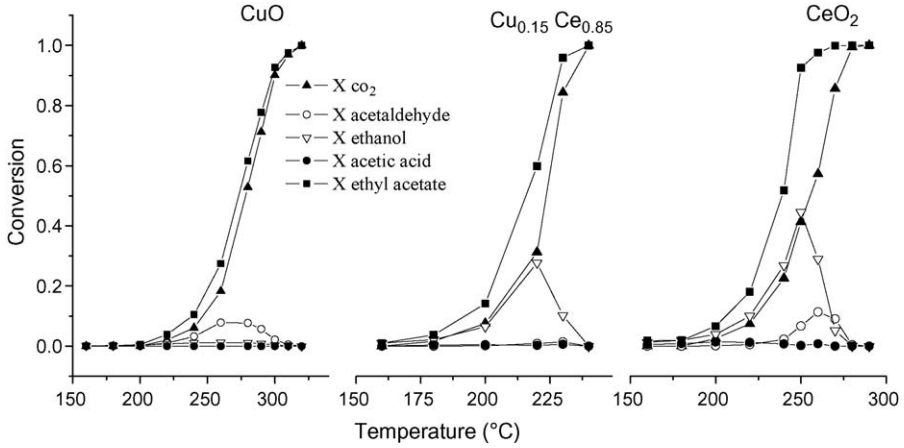

Fig. 8. Intermediate products of ethyl acetate oxidation over CeO_2, $Cu_{0.15}Ce_{0.85}$ and CuO catalysts.

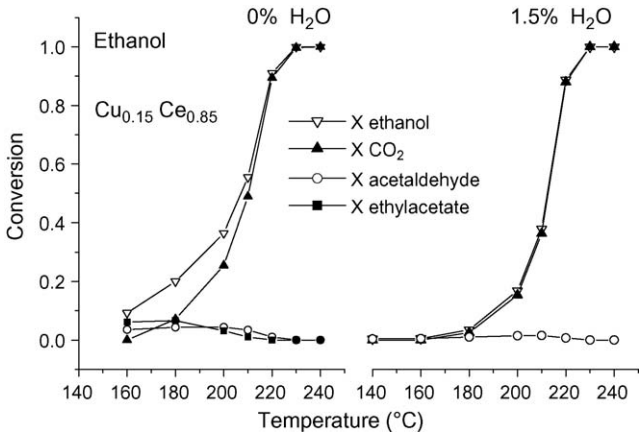

Fig. 9. Effect of water on ethanol oxidation over the $Cu_{0.15}Ce_{0.85}$ catalyst.

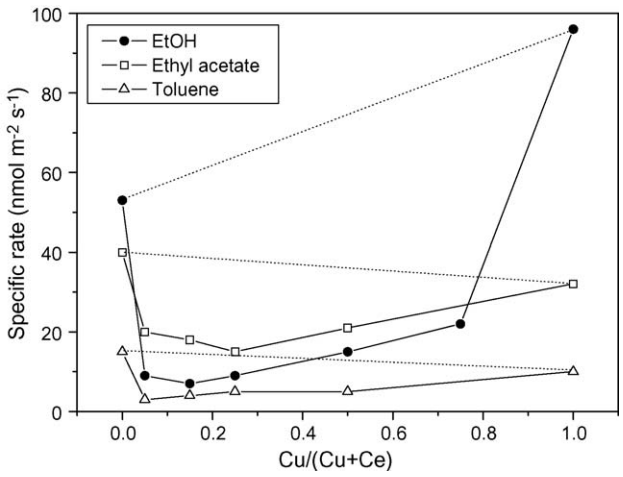

Fig. 11. Specific activity (specific rate of VOC consumption) as a function of Cu/(Cu + Ce) ratio.

$Cu_{0.15}Ce_{0.85}$ catalyst. Regarding the effect of CO_2, it was found that addition of up to 20% CO_2 has a negligible effect on catalytic activity, and the temperature required for complete conversion of ethanol does not change. The presence of 1.5% H_2O in the feed causes a moderate decrease in catalyst activity, which is more pronounced during ethyl acetate oxidation. The conversion of ethanol decreases at low reaction temperatures in the presence of water, but the temperature required for complete conversion of ethanol remains the same. In the case of ethyl acetate oxidation, the temperature required for complete conversion to CO_2 is shifted by 10 °C to higher temperatures in the presence of water. The presence of H_2O causes a marked decrease of the intermediate products of ethanol oxidation, as it can be seen in Fig. 9. The maximum concentration of acetaldehyde was 80 ppm in the absence of water and only 15 ppm in the presence of H_2O (ethanol feed of 1600 ppm in both cases). A less pronounced decrease in the yield of acetaldehyde (from 31% to 19%) in the presence of water has been also reported in Ref. [1] for $CuO–CeO_2/TiO_2$ catalysts. The presence of water enhances slightly the conversion of ethyl acetate to ethanol and acetic acid at low reaction temperatures, due to the promoting effect of water on the hydrolysis reaction (Fig. 10). In the case of toluene oxidation, the presence of 1.5% H_2O in the feed has an inhibiting effect and the temperature required for complete conversion of toluene is increased by 30 °C (300 °C vs. 270 °C in the absence of water). A negative effect of water addition on toluene oxidation over CuO/CeO_2 and $CuO/\gamma–Al_2O_3$ catalysts, has been also reported by Wang et al. [40].

The activity of Cu_xCe_{1-x} catalysts in the oxidation of ethanol, ethyl acetate and toluene is higher than the one of pure CuO and

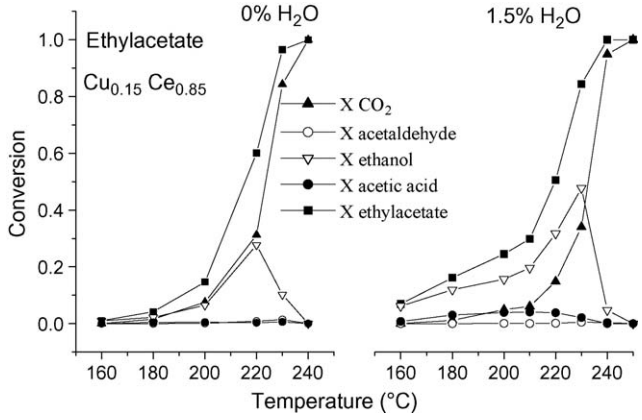

Fig. 10. Effect of water on ethyl acetate oxidation over the $Cu_{0.15}Ce_{0.85}$ catalyst.

CeO_2 catalysts, as has been shown in Figs. 4–6. Calculation of differential reaction rates on a unit mass basis (e.g., nmol g^{-1} s^{-1}) shows that Cu_xCe_{1-x} catalysts are generally 2–10 times more active than the corresponding pure oxides. However, Cu_xCe_{1-x} catalysts have significantly higher surface area than the pure oxides (Table 2) and a more meaningful comparison can be made by employing the specific activity calculated per unit surface area of the catalysts. Fig. 11 presents the specific activity (specific rate of VOC consumption) of all catalysts (units: nmol m^{-2} s^{-1}) in the oxidation of ethanol, ethyl acetate and toluene, as a function of the Cu/(Cu + Ce) atomic ratio. The dashed lines in Fig. 11 correspond to the expected activity of a $CuO–CeO_2$ physical mixture. Due to the fact that any specific catalyst shows different activity in the oxidation of the three examined compounds, the specific activity has been calculated at different temperatures: 200 °C for ethanol, 220 °C for ethyl acetate and 240 °C for toluene. Regarding the pure oxides, the specific activity of CuO is higher than the one of CeO_2 in ethanol oxidation, but lower in ethyl acetate and toluene oxidation. In all cases, Cu_xCe_{1-x} catalysts exhibit lower specific activities than those of pure CuO and CeO_2 oxides. Regarding ethanol oxidation, the specific activity of CuO is 96 nmol m^{-2} s^{-1}, of CeO_2 is 53 nmol m^{-2} s^{-1}, while specific activities of Cu_xCe_{1-x} catalysts are in the range of 7–22 nmol m^{-2} s^{-1}. It should be noted that the lowest value corresponds to the $Cu_{0.15}Ce_{0.85}$ catalyst, while further increase of copper content is accompanied by increase of specific activity. The same trend is observed during ethyl acetate and toluene oxidation, as the increase of copper content leads to an increase of specific activity. In the case of ethyl acetate oxidation, the specific activities of pure oxides are 40 nmol m^{-2} s^{-1} for CeO_2 and 32 nmol m^{-2} s^{-1} for CuO, while specific activities of Cu_xCe_{1-x} catalysts are in the range of 15–21 nmol m^{-2} s^{-1}. In the case of toluene oxidation, the specific activities of all Cu_xCe_{1-x} catalysts are in the range of 3–5 nmol m^{-2} s^{-1} compared to 15 nmol m^{-2} s^{-1} for CeO_2 and 10 nmol m^{-2} s^{-1} for pure CuO. These results show that the superior performance of Cu_xCe_{1-x} catalysts compared to pure CuO and CeO_2, is due to their higher specific surface areas, which overcompensate their lower specific activity.

The apparent activation energies, E_{app}, of CO_2 formation during ethanol, ethyl acetate and toluene oxidation over Cu_xCe_{1-x} catalysts are presented in Table 3. The apparent activation energies and prefactors were calculated from Arrhenius plots using the specific rate of CO_2 production expressed on a unit surface area basis (nmol m^{-2} s^{-1}). The temperature range employed in these calculations was the one corresponding to less than 20% VOC

Table 3
Apparent activation energies (kJ mol^{-1}) of CO_2 formation during VOC oxidation.

Catalyst	Ethanol	Ethyl acetate	Toluene
CeO_2	85 ± 6	111 ± 7	65 ± 12
$Cu_{0.05}Ce_{0.95}$	101 ± 17	134 ± 16	83 ± 5
$Cu_{0.15}Ce_{0.85}$	123 ± 8	145 ± 29	83 ± 8
$Cu_{0.25}Ce_{0.75}$	104 ± 27	128 ± 14	84 ± 7
$Cu_{0.5}Ce_{0.5}$	123 ± 17	140 ± 7	82 ± 4
$Cu_{0.75}Ce_{0.25}$	121 ± 11	nd	nd
CuO	136 ± 15	121 ± 9	120 ± 16

conversion to CO_2. The apparent activation energies vary from 65 kJ mol^{-1} (toluene on CeO_2) to 145 kJ mol^{-1} (ethyl acetate on $Cu_{0.15}Ce_{0.85}$). The apparent activation energies measured over Cu_xCe_{1-x} catalysts for ethanol and toluene oxidation get intermediate values in the range defined by the values measured over the CeO_2 and CuO catalysts. In the case of ethyl acetate oxidation, the apparent activation energies over Cu_xCe_{1-x} catalysts are slightly higher than over pure oxides. The Constable plot of apparent activation energies, E_{app}, of the reactions of ethanol, ethyl acetate and toluene oxidation over Cu_xCe_{1-x} catalysts is presented in Fig. 12. All data fit into the Cremer–Constable relation ($\ln A_{app} = \alpha E_{app} + b$), i.e. a compensation effect is present. The temperature range in which measurements were carried out was 160–280 °C. Assuming an average temperature of 220 °C, the $(RT)^{-1}$ term is 0.244 mol kJ^{-1}, which is very close with the slope α of the Constable plot, which was determined to be 0.251 mol kJ^{-1}, in agreement with the analysis of Lynggaard et al. [41]. It should be mentioned that a compensation effect was also found during oxidation of ethanol, ethyl acetate and toluene oxidation over Mn_xCe_{1-x} catalysts [11].

3.4. Overview

Interaction of CuO and CeO_2 already manifests itself during synthesis of the catalysts, as the presence of both oxides leads to materials with higher surface area than the pure oxides. Crystallite growth of one phase is obviously inhibited by the presence of the second phase. A similar effect was also observed for combustion-prepared MnO_x–CeO_2 materials [11]. This phenomenon appears to be generally operative when both phases are formed simultaneously, as, for example, in the case of CuO–CeO_2 catalysts prepared by a citrate method [42]. Copper oxide is segregated on the surface of ceria, as has been shown by XPS measurements [12,42], and ceria acts to efficiently stabilize copper oxide dispersion. Copper is present in the form of CuO clusters, copper ions incorporated in the surface layer of ceria, as well as larger CuO particles depending on copper content. CuO–CeO_2 catalysts have been extensively studied mostly due to their high activity in (selective) CO oxidation, which has been mainly attributed to the enhanced reducibility of the catalytic surface. We have previously reported that the specific activity (per unit surface area of catalyst) of CuO–CeO_2 catalysts in CO oxidation is up to four times higher than the one of pure CuO [42]. It is obvious, on the other hand, that a positive effect of enhanced reducibility on VOC oxidation activity is not present, as the specific activity of CuO–CeO_2 in VOC oxidation is lower than the one of pure CuO or CeO_2. This result implies that the catalytic sites, which are responsible for the high activity in CO oxidation, are not operative under conditions of VOC oxidation. CO oxidation proceeds via addition of lattice oxygen to an adsorbed CO molecule. On the other hand, oxidation of VOCs proceeds via a more complicated pathway. Taking ethanol as an example, its oxidation involves its adsorption on the surface and subsequent breaking of a number of C–H and O–H bonds and of one C–C bond. Due to the energetic requirements of the reaction, the examined catalysts are approximately four orders of magnitude less active in ethanol oxidation than in CO oxidation. An additional remark is that the specific activity of CuO–CeO_2 catalysts increases with decrease of their surface area. This is shown in Fig. 13, which presents the specific activity of $Cu_{0.15}Ce_{0.85}$ catalysts with varying surface area prepared with different urea equivalence ratios (Table 1). It can be observed that the specific activity of the $Cu_{0.15}Ce_{0.85}$ catalyst increases from 6 to ~20 nmol m^{-2} s^{-1} with decrease of surface area from 53 to 10 m^2 g^{-1}. The specific activity of CeO_2, however, is still higher than the one of the most active $Cu_{0.15}Ce_{0.85}$ catalyst, as shown in Fig. 13. The observed trend is indicative of structure sensitivity of the reaction of ethanol oxidation, i.e. intrinsic activity increases with decrease of surface area, which corresponds to increase of crystallite size and decrease of dispersion of oxide phases. Therefore, the lower specific activity of Cu–Ce catalysts can be partially attributed to such a surface area effect. It should be noted that the observed behavior of CuO–CeO_2 catalysts is similar to that reported recently by us for MnO_x–CeO_2 catalysts in VOC oxidation [11], where it was found that the specific activity of mixed oxide catalysts is lower than the one of pure oxides and the specific activity decreases with increase of surface area.

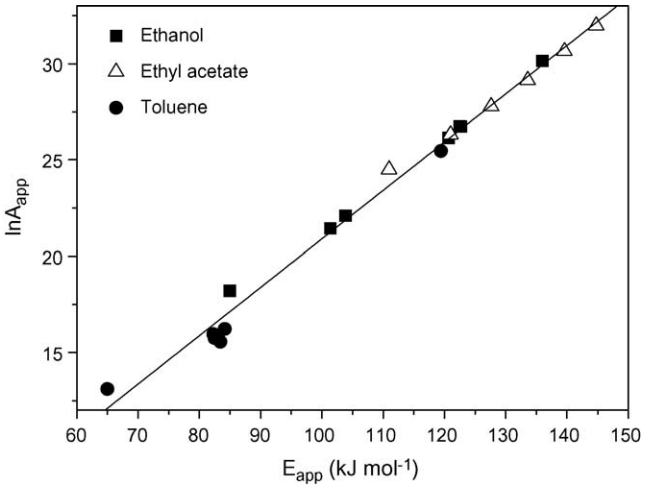

Fig. 12. Constable plot of apparent prefactors as a function of apparent activation energies for the specific rate of CO_2 production during oxidation of ethanol, ethyl acetate and toluene over Cu_xCe_{1-x} catalysts.

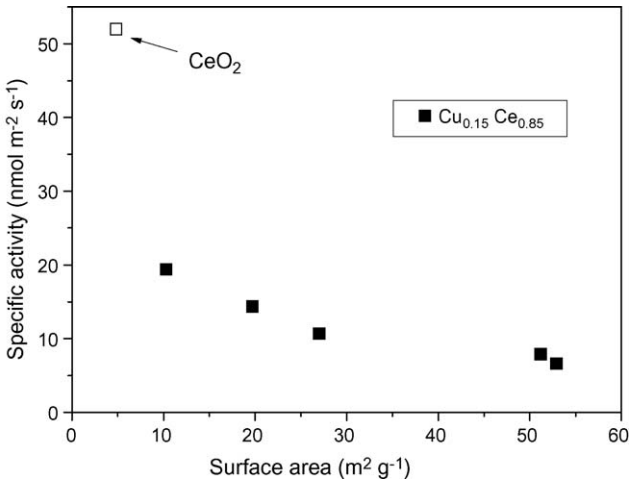

Fig. 13. Specific activity (specific rate of ethanol consumption) as a function of the surface area of the $Cu_{0.15}Ce_{0.85}$ catalyst.

Ethanol oxidation over the examined catalysts proceeds according to a series reaction scheme. Ethanol gets initially oxidized to acetaldehyde which subsequently gets oxidized to CO_2. The presence of ethyl acetate in the reaction products indicates that acetaldehyde oxidation proceeds via formation of surface acetate species. This reaction scheme appears to be generally valid for copper-containing catalysts [1,43]. Cu_xCe_{1-x} catalysts produce considerably less acetaldehyde than the pure oxides. In comparison to Mn–Ce catalysts [11], they are less active, but also less selective to formation of acetaldehyde and their performance is improved even further in the presence of water. To the best of our knowledge, the $Cu_{0.15}Ce_{0.85}$ catalyst offers probably the lowest acetaldehyde selectivity ever reported during ethanol oxidation. The low selectivity of Cu_xCe_{1-x} catalysts towards acetaldehyde indicates that the specific rate of ethanol consumption over these catalysts (as compared to pure oxides, Fig. 11) is decreased to a greater extent compared to the specific rate of CO_2 production. At the temperature of 200 °C, the specific rate of CO_2 production over Cu_xCe_{1-x} catalysts is three times lower than the one of pure CeO_2. On the other hand, Cu_xCe_{1-x} catalysts have higher specific rates of CO_2 production than pure CuO, which produces almost no CO_2 at this temperature.

Oxidation of ethyl acetate proceeds with initial hydrolysis to ethanol and acetic acid. Acetic acid is preferentially oxidized with respect to ethanol due to its stronger binding on the catalyst surface [11], while ethanol gets oxidized to CO_2 via acetaldehyde. Cu_xCe_{1-x} catalysts produce extremely low amounts of acetaldehyde during ethylacetate oxidation both in the presence and absence of water in analogy to what was found in ethanol oxidation.

4. Conclusions

CuO–CeO_2 mixed oxides – prepared by a combustion method – have higher surface areas than the corresponding pure oxides and are efficient total oxidation catalysts allowing destruction of ethanol and ethylacetate with minimal formation of undesired by-products (acetaldehyde) at all conversion levels. In contrast to CO oxidation, the specific activity of Cu_xCe_{1-x} catalysts in the oxidation of ethanol, ethylacetate and toluene is lower than the one of pure CuO and CeO_2, i.e. combination of the two phases leads to suppression of intrinsic activity. Nevertheless, mixed catalysts achieve complete VOC conversion at lower temperatures because of their higher surface area. Ethanol oxidation over $Cu_{0.15}Ce_{0.85}$ appears to be structure sensitive, as the specific reaction rate increases with decrease of catalyst surface area. Pure CuO produces only acetaldehyde at low reaction temperatures, while CeO_2 produces lower amounts of acetaldehyde than CuO. Combination of CuO with CeO_2 leads to catalysts offering considerably lower selectivity to acetaldehyde than the pure oxides, which is due to the fact that the specific rate of ethanol consumption decreases to a greater extent than the specific rate of CO_2 production. Actually, the specific rate of CO_2 production over Cu_xCe_{1-x} catalysts is higher than the one over CuO, which does not produce any CO_2 at low reaction temperatures.

References

[1] P.-O. Larsson, A. Andersson, J. Catal. 179 (1998) 72.
[2] P. Papaefthimiou, T. Ioannides, X.E. Verykios, Appl. Therm. Eng. 18 (1998) 1005.
[3] G. Avgouropoulos, E. Oikonomopoulos, D. Kanistras, T. Ioannides, Appl. Catal. B: Environ. 65 (2006) 62.
[4] P. Papaefthimiou, T. Ioannides, X.E. Verykios, Catal. Today 54 (1999) 81.
[5] F.J. Maldonado-Hódar, C. Moreno-Castilla, A.F. Perez-Cadenas, Appl. Catal. B: Environ. 54 (2004) 217.
[6] H.L. Tidahy, S. Siffert, F. Wyrwalski, J.-F. Lamonier, A. Aboukaïs, Catal. Today 119 (2007) 317.
[7] K. Everaert, J. Baeyens, J. Hazard. Mater. B 109 (2004) 113.
[8] S. Scirè, S. Minicò, C. Crisafulli, S. Galvagno, Catal. Commun. 2 (2001) 229.
[9] H. Rotter, M.V. Landau, M. Carrrera, D. Goldfarb, M. Herskowitz, Appl. Catal. B: Environ. 47 (2004) 111.
[10] S.C. Kim, J. Hazard. Mater. B 91 (2002) 285.
[11] D. Delimaris, T. Ioannides, Appl. Catal. B: Environ. 84 (2008) 303.
[12] G. Avgouropoulos, T. Ioannides, Appl. Catal. A: Gen. 244 (2003) 155.
[13] W. Liu, M. Flytzani-Stephanopoulos, J. Catal. 153 (1995) 317.
[14] W. Liu, A.F. Sarofim, M. Flytzani-Stephanopoulos, Chem. Eng. Sci. 49 (1994) 4871.
[15] T. Tabakova, V. Idakiev, J. Papavasiliou, G. Avgouropoulos, T. Ioannides, Catal. Commun. 8 (2007) 101.
[16] P. Bera, S.T. Aruna, K.C. Patil, M.S. Hegde, J. Catal. 186 (1999) 36.
[17] G.R. Rao, H.R. Sahu, B.G. Mishra, Colloid Surf. A 220 (2003) 261.
[18] S. Hocevar, J. Batista, J. Levec, J. Catal. 184 (1999) 39.
[19] J. Xiaoyuan, L. Guanglie, Z. Renxian, M. Jianxin, C. Yu, Z. Xiaoming, Appl. Surf. Sci. 173 (2001) 208.
[20] X.-C. Zheng, S.-H. Wu, S.-P. Wang, S.-R. Wang, S.-M. Zhang, W.-P. Huang, Appl. Catal. A: Gen. 283 (2005) 217.
[21] P. Bera, K.R. Priolkar, P.R. Sarode, M.S. Hegde, S. Emura, R. Kumashiro, N.P. Lalla, Chem. Mater. 14 (2002) 3591.
[22] S.M. Zhang, W.P. Huang, X.H. Qiu, B.Q. Li, X.C. Zheng, S.H. Wu, Catal. Lett. 80 (2002) 41.
[23] C. Hu, Q. Zhu, Z. Jiang, Y. Zhang, Y. Wang, Micropor. Mesopor. Mater. 113 (2008) 427.
[24] H.P. Klug, L.E. Alexander, X-ray Diffraction Procedures, second ed., Wiley, New York, 1974, p. 642.
[25] D.A.M. Monti, A. Baiker, J. Catal. 83 (1983) 323.
[26] P. Malet, A. Caballero, J. Chem. Soc., Faraday Trans. 84 (1988) 2369.
[27] M.F. LuO, J.M. Ma, J.Q. Lu, Y.P. Song, Y.J. Wang, J. Catal. 246 (2007) 52.
[28] X.L. Tang, B.C. Zhang, Y. Li, Y.D. Xu, Q. Xin, W.J. Shen, Catal. Today 93 (2004) 191.
[29] G. Avgouropoulos, T. Ioannides, H. Matralis, Appl. Catal. B: Environ. 56 (2005) 87.
[30] S. Zhang, W. Huang, X. Qiu, B. Li, X. Zheng, S. Wu, Catal. Lett. 80 (2002) 41.
[31] S. Hocevar, U.O. Krasovec, B. Orel, A.S. Arico, H. Kim, Appl. Catal. B: Environ. 28 (2000) 113.
[32] J.B. Wang, D.H. Tsai, T.J. Huang, J. Catal. 208 (2002) 370.
[33] F. Marino, B. Schönbrod, M. Moreno, M. Jobbagy, G. Baronetti, M. Laborde, Catal. Today 133–135 (2008) 735.
[34] C.R. Jung, J. Han, S.W. Nam, T.-H. Lim, S.-A. Hong, H.-I. Lee, Catal. Today 93–95 (2004) 183.
[35] M. Ferrandon, J. Carno, S. Jaras, E. Bjornbom, Appl. Catal. A: Gen. 180 (1999) 141.
[36] A. Pintar, J. Batista, S. Hocevar, J. Colloid Interf. Sci. 285 (2005) 218.
[37] W. Liu, M. Flytzani-Stephanopoulos, Chem. Eng. J. 64 (1996) 283.
[38] X. Zheng, X. Zhang, X. Wang, S. Wang, S. Wu, Appl. Catal. A: Gen. 295 (2005) 142.
[39] T. Caputo, L. Lisi, R. Pirone, G. Russo, Appl. Catal. A: Gen. 348 (2008) 42.
[40] C.-H. Wang, S.-S. Lin, C.-L. Chen, H.-S. Weng, Chemosphere 64 (2006) 503.
[41] H. Lynggaard, A. Andreasen, C. Stegelmann, P. Stoltze, Prog. Surf. Sci. 77 (2004) 71.
[42] G. Avgouropoulos, T. Ioannides, Appl. Catal. B: Environ. 67 (2006) 1.
[43] M.R. Morales, B.P. Barbero, L.E. Cadus, Fuel 87 (2008) 1177.